High sensitivity liquid level sensor for microfluidic applications using a hollow core fiber structure

doi: info:doi/10.1016/j.sna.2021.113134

High sensitivity liquid level sensor for microfluidic applications using a hollow core fiber structure

Dejun Liu,[1] Wei Li, [1] Qiang Wu,[2,3] Haoyu Zhao,[4] Fengzi Ling, [1] Ke Tian,[5] Changyu Shen,[6] Wei Han,[7] Fangfang Wei,[7] Gerald Farrell,[7] Yuliya Semenova,[7] and Pengfei Wang[1,8,*]

[1]*Key Laboratory of Optoelectronic Devices and Systems of Ministry of Education and Guangdong Province, College of Physics and Optoelectronic Engineering, Shenzhen University, Shenzhen, 518060, China*
[2]*Key Laboratory of Nondestructive Test (Ministry of Education), Nanchang Hangkong University, Nanchang 330063, China*
[3]*Department of Mathematics, Physics and Electrical Engineering, Northumbria University, Newcastle Upon Tyne, NE1 8ST, United Kingdom*
[4]*Technical Center, Sichuan Changhong Electric Co., Ltd, Mianyang, 621000, China*
[5]*Okinawa Institute of Science and Technology Graduate University, Onna, Okinawa 904-0495, Japan*
[6]*Institute of Optoelectronic Technology, China Jiliang University, Hangzhou, 310018, China*
[7]*Photonics Research Centre, Technological University Dublin, Kevin Street, Dublin 8, Ireland*
[8]*Key Lab of In-fiber Integrated Optics, Ministry Education of China, Harbin Engineering University, Harbin 150001, China*

*E-mail: pengfei.wang@tudublin.ie

Abstract: Liquid level measurement in microfluidics is challenging, where a sensor with ultra-high sensitivity but miniature in nature is demanded. In this paper, we propose for the first time a microsized fiber sensor structure in both diameter and length for microfluidics applications, which is capable of sub-micrometer scale liquid level measurement. The sensor is simply fabricated by fusion splicing a short section of a hollow core fiber (HCF) between two singlemode fibers (SMFs). HCFs with different air core diameters (10 μm, 20 μm, 30 μm) were investigated and it is found that for a given length of HCF stronger resonant dips were excited in transmission for the HCF with a smaller air core diameter. Thus the HCF structure with an air core diameter of 10 μm (HCF-10) was used for demonstration of high sensitivity liquid level measurement in microfluidics. Simultaneous excitation of both Anti-Resonant Reflecting Optical Waveguide (ARROW) guiding mechanism and Mach-Zehnder interferometer (MZI) in transmission is demonstrated in such an HCF-10 structure when HCF-10 is longer than the critical length. A maximum sensitivity of 0.042 dB/μm (corresponding to a calculated liquid level resolution of ~0.23 μm) was experimentally achieved with an HCF-10 length of ~867 μm, which is three times higher than that of the previous reported to date of the most sensitive fiber optic liquid level sensors based on intensity modulation. In addition, the proposed sensor shows good repeatability of measurement and a very low cross sensitivity to changes in the surrounding refractive index.

Key words: Fiber sensor, hollow core fiber, antiresonant, Mach-Zehnder interferometer, liquid level

1. Introduction

Microfluidics is a technology that manipulates fluids in a microchannel with typical dimensions ranging from hundreds of nanometers to hundreds of micrometers. It offers great advantages such as small size, fast analysis, small footprints for the analytical devices, very small quantities of reagents consumed and high level of functional integration for applications. Microfluidics has driven significant advances and innovations in various fields such as

molecular analysis, molecular biology, microelectronics, food analysis and point-of-care diagnostics [1-3].

Liquid level measurement in microfluidics is essential, where accurate control of the volume of the fluids in a range from attoliters (10^{-18} liter) to nanoliters (10^{-9} liter) is required [2]. A fiber optic sensor could be a good candidate to be used in microfluidics for monitoring liquid level variations due to its inherent advantages such as miniature size, non-metallic nature (non-conductive), immunity to electromagnetic interference, high resistance to corrosion, and remote sensing capability. Recently, several optical fiber based lab-on-a-chip (LOC) devices or lab-on-a-fiber (LOF) devices have been reported. For example, Lin et al. proposed an optofluidic waveguide coupler in fiber for discrimination of gutter oil from healthy vegetable oil [4]. Gao et al. reported an optofluidic immunosensor based on a hollow core fiber structure [5].

In the past few decades, a number of fiber structures based on fiber gratings and fiber interferometer configurations have been proposed for liquid level measurement and some of them have achieved very high sensitivities and high resolutions [6-13]. For example, Yan et at. proposed a water level sensor based on a tilted fiber grating structure with a sensitivity of 3.06 dB/mm [6]. Antonio-Lopez demonstrated a liquid level sensor by using a reflective no core fiber structure, the sensitivity of which varies from 0.17 nm/mm to 0.57 nm/mm depending on the surrounding refractive index (SRI) of the liquid [7]. Wang et al. reported an ultra-high liquid level sensitivity of 367.644 nm/mm sensor based on a tapered fiber structure [8]. However, the application of above sensor structures is limited due to their high sensitivities to variations in the SRI value of the liquid in use. In addition, the fiber sensor structures above are miniature in diameter but have relatively large length scale ranging from millimeters to centimeters along the longitude direction, which means that such sensors are not suitable to be used in microfluidics devices where sensor heads with micrometers length or less are required. Most recently, we have reported a highly sensitive liquid level sensor based on an anti-resonant (AR) hollow core fiber (HCF, air core diameter ~30 μm, sensor head length ~4.7 mm) with a maximum sensitivity of 0.014dB/μm [14]. It is demonstrated that the HCF based sensor structure is not sensitive to the change of SRI. However, the resonant dip strength decreased significantly with reductions in the length of HCF and it disappeared when the HCF length was shortened to ~1 mm, thus it cannot be used in microfluidics application. Overall then for fiber interferometers, it remains a challenge to fabricate a liquid level sensor structure at a length scale of micrometers while maintaining a high sensitivity.

In this paper, we propose for the first time a micrometer length liquid level sensor fabricated by fusion splicing a short section of HCF, with a small air core diameter of 10 μm (HCF-10), between two singlemode fibers (SMFs). Both Anti-Resonant Reflecting Optical Waveguide (ARROW) and Mach-Zehnder interferometer (MZI) guiding mechanisms are simultaneously excited in transmission in such a small (comparable to the core diameter of an SMF) air core HCF structure when the HCF was longer than the critical length. The resonant dips produced by ARROW were used to monitor the changes of a liquid level based on an intensity modulation scheme. A maximum liquid level sensitivity of 0.042 dB/μm was experimentally achieved for the sensor with an HCF length of 867 μm, which is three times higher than that of the previously reported most sensitive fiber optic liquid level sensors based on intensity modulation to date. In addition, it is demonstrated that the proposed sensor shows good repeatability of measurement and a very low cross sensitivity to changes in SRI. Since the sensor structure is only hundreds of micrometers in both diameter and length, it is suitable for liquid level measurement in microfluidics. It is noted that compared to our previous work [14], in this study we have achieved a more compact sensor structure and higher liquid level sensitivities using a smaller air core diameter based HCF. Light transmission mechanism of the proposed HCF-10 structure in this study is also different from that of the previous one.

2. Experimental setup

HCFs with the same outer silica cladding diameter of ~126 µm and different air core diameters of ~10 µm, ~20 µm and~30 µm were used in the experiment. The HCFs were denoted as HCF-10, HCF-20, and HCF-30 with the number representing the air core diameter. The proposed liquid level sensor structure was fabricated by fusion splicing a short section of an HCF between two SMFs as illustrated in Fig. 1(a). The splicing parameters were carefully managed to avoid the collapse of the air core. In particular, a Fujikura 62S+ was used and an automatic splicing mode was applied with an arc power of -75 bit and an arc time of 600 microseconds. Figure 1(b) and (c) show a few microscope images of the prepared HCF structures with different length of HCF and a schematic diagram of the experimental setup for the liquid level measurement. Since the monitored liquid level changes were in the order of micrometers, in our experiment all liquid level variations were measured with the help of an optical microscope as a reference. The prepared sensor structure was inserted into a transparent plastic test tube with its two SMF ends fixed on two stages, liquids were pumped into the test tube at a speed of 2 r/min by a peristaltic pump (Baoding Qili Precision Pump Cooperation, BT100-02) which can control both the liquid flow direction and speed. A soft tube with an inner air core diameter of 900 µm was used in the pump to achieve a stable and low speed liquid input. For a better control of the flow speed of the liquid, a test tube with a relatively large diameter (inner diameter ~3 mm) was chosen, a small slot was cut on the test tube to provide a better view for the microscope. Since the slot size was small, no obvious influence on the flow of liquids was observed. Light from a broadband supercontinuum source (SC, SC-YSL) was launched into the HCF based sensor structure and the transmitted light was interrogated by an optical spectrum analyzer (OSA, Yokogawa AQ6370D).

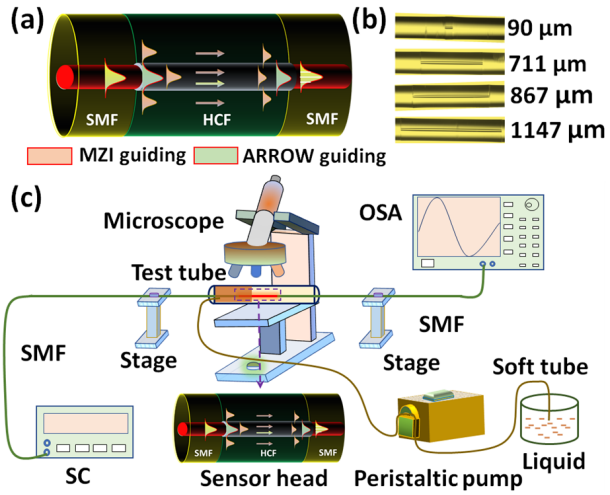

Fig. 1. (a) A schematic diagram of the proposed HCF structure; (b) Microscopic images of the prepared sensor structures with different HCF lengths; (c) The experimental setup for liquid level measurement.

3. Theoretical analysis

Since the RI of the air core is smaller than that of the silica cladding, guidance of light through total internal reflection as in conventional fibers is not applicable in an HCF. Its guiding mechanism could be understood with the ARROW model, in which the outer silica cladding acts like a pair of FP etalons, where only certain wavelengths which meet the anti-resonance condition in the silica cladding, are confined and transmitted inside the air core.

The resonant wavelength (λ_m^{AR}) and free spectral range (FSR) can be predicted with the following equations [15]:

$$\lambda_m^{AR} = \frac{2t}{m}\sqrt{n_{\text{clad}}^2 - n_{core}^2} \tag{1}$$

$$FSR_{AR} = \frac{\lambda_m \lambda_{m+1}}{2t\sqrt{n_{clad}^2 - n_{core}^2}} \tag{2}$$

where λ_m and λ_{m+1} are the central wavelengths of the two adjacent transmission dips, n_{clad} and n_{core} are the refractive indices of silica cladding and air core of HCF. t is the thickness of the silica cladding and m is the resonance order (it is a nonnegative integer). For a SMF-HCF-SMF structure, it is important to know that ARROW guidance is excited only if the length of HCF is longer than the critical length (L_c), which is given as [16]:

$$L_c = \sqrt{n_{core}^2 + n_{clad}^2 - n_{smf}^2}\left(\frac{r}{\sqrt{n_{smf}^2 - n_{clad}^2}} + \frac{2t}{\sqrt{n_{smf}^2 - n_{core}^2}}\right) \tag{3}$$

where n_{smf} is the RI of the SMF core, r is the radius of the hollow core.

The strength of resonant dip produced by ARROW effect is dependent on the length of the HCF. A longer HCF section produces stronger dips in the transmission spectrum [14]. As can be seen from Eq. (3), L_c decreases with the decrease of the air core diameter. For a given length, HCF with a smaller air core diameter experiences a greater number of reflections and hence produces stronger dips in transmission. The experimental demonstration is shown in Fig. 2. Three types of HCFs with different air core diameters (10 μm, 20 μm, 30 μm) and lengths were investigated. Strong ARROW resonant dips could only be found in the transmission spectrum of HCF-10 structure when the lengths of sensor heads were decreased to ~1 mm. Thus only the HCF-10 structure is suitable for monitoring changes of liquid level in microfluidics where sensor heads with micrometers length or less are required.

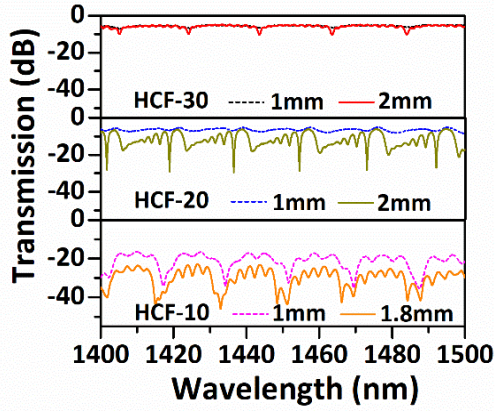

Fig. 2. Measured transmission spectra in air for HCF based fiber structures with different air core diameters and HCF lengths.

It has been reported that an MZI guiding mechanism is excited when the core diameter of an HCF and a SMF are comparable [17]. Since the leakage loss in an HCF increases as the air core diameter decreases [18], more light leaks into the silica cladding for a smaller air core diameter HCF, light propagating in the air core and silica cladding interfere with each other at the end of HCF, which is collected by the output SMF, thus an MZI is formed. The MZI can be explained with a "two-beam optical interference model", where the resonant dips (λ_m^{MZ}) in the transmission spectrum can be derived as [19]:

$$\lambda_m^{MZ} = 2\triangle n_{eff} L / (2m+1) \quad (4)$$

where Δn_{eff} is the difference between the effective refractive indices of the two interfering modes and L is the length of the sensor head. The corresponding FSR between any two adjacent transmission dips can be described by the formula:

$$FSR_{MZI} = \frac{\lambda_m \lambda_{m+1}}{\triangle n_{eff} L} \quad (5)$$

To investigate the light guiding mechanism in the proposed HCF-10 structure, the transmission and reflection spectral responses in air and water for different lengths of the HCF-10 were recorded as displayed in Fig. 3. A total of seven sensors where fabricated with lengths of 90, 254, 711, 867, 996, 1147 and 1807 μm. Each sensor was given a reference name denoted as S-90, S-254, S-711, S-867, S-996, S-1147 and S-1807, with the number signifying the HCF section length in micrometer. The reflection spectra were measured with the help of a circulator. For the sake of brevity, the experimental setup is not shown here, similar setup could be found in a previous report [20]. Periodic dips can be seen in the reflection spectra (shown in dashed line in Fig. 3), the dips' strength and FSR of which gradually decrease with an increase in the HCF length. No obvious dips are observed in the reflection spectrum when the HCF length reaches 711 μm, thus the reflection spectra for the sensors with longer HCF lengths than 711 μm were not measured in the experiment. The reflection spectra are easy to understand given the effect of a Fabry-Perot interferometer (FPI) produced by the two air/silica interfaces between the SMFs and HCF. For an FPI, the central wavelength of the reflection dips (λ_m^{FP}) and the FSR_{FP} between any two adjacent dips can be expressed as [21]:

$$\lambda_m^{FP} = \frac{4L}{2m+1} n_{core} \quad (6)$$

$$FSR_{FP} = \frac{\lambda_m \lambda_{m+1}}{2n_{core} L} \quad (7)$$

All above equations are summarized for clarity in Table 1 to provide a comparison between different guiding mechanisms.

Table 1. Equations for the calculation of spectral resonant dips' wavelength and their corresponding FSRs of different light guiding mechanisms.

Guiding mechanism	λ_m	FSR
ARROW	$\frac{2t}{m}\sqrt{n_{\text{clad}}^2 - n_{core}^2}$	$\frac{\lambda_m \lambda_{m+1}}{2t\sqrt{n_{clad}^2 - n_{core}^2}}$
MZI	$\frac{2}{(2m+1)}\triangle n_{eff} L$	$\frac{\lambda_m \lambda_{m+1}}{\triangle n_{eff} L}$
FP	$\frac{4L}{2m+1} n_{core}$	$\frac{\lambda_m \lambda_{m+1}}{2Ln_0}$

Taking sensor sample S-90 as an example, the measured FSR of reflection spectrum at 1500 nm is ~12.76 nm, L is thus calculated to be ~88 μm, which is very close to the experimental measured value of ~90 μm. Based on Eqs. (6) and (7), the dip positions and the FSR are independent of the SRI, thus as expected the reflection spectra of the sensor structure show no changes in water compared to those in air. In contrast to the reflection spectra, dips with higher strength and larger FSR are observed in the transmission spectra as shown in Fig. 3(a) and (b), indicating that a different light guiding mechanism is involved in the transmission.

Jung *et al.* [17] were the first to report that an MZI was formed in a small air core HCF structure with a diameter of 9 μm, but no sign of ARROW guidance was found in the transmission spectra since only very short lengths of HCF (less than 200 μm) were investigated in their study. Zhang *et al.* [16] investigated the transition of FP and ARROW mechanisms in an HCF structure, it was found that anti-resonant guidance can be excited in reflection for an HCF with a relatively large air core (larger than 20 μm) when HCF is longer than L_c. In this work, an HCF with a critical air core diameter of 10 μm was selected and simultaneous excitation of both ARROW and MZI guiding mechanism were experimentally demonstrated in transmission in HCF-10 when the HCF length is longer than L_c. For a given HCF-10, assuming n_{smf} , n_{clad} and n_{core} are 1.455, 1.45 and 1.0 respectively, r and t are 5 μm and 58 μm. According to Eq. (3), L_c is calculated to be ~191 μm. Therefore no resonant dips are observed in the transmission spectrum for the sample S-90 as shown in Fig. 3(a). For a sensor structure which has an HCF length longer than L_c, its transmission spectrum is a hybrid spectrum resulting from both ARROW and MZI guiding mechanisms. For sample S-254, the effect of ARROW is weak, the resonant dips are not obvious. As the length of the HCF further increases, strong periodic dips appear with their dips' central wavelengths almost fixed. The experimentally measured FSRs of the strong dips at 1500 nm of S-711, S-867 and S-996 are 18.43 nm, 18.74nm, 17.47 nm, respectively, which matches very well with the calculated value of 18.33 nm using Eq. 2. It is thus concluded that those periodic strong dips are produced by the ARROW effect.

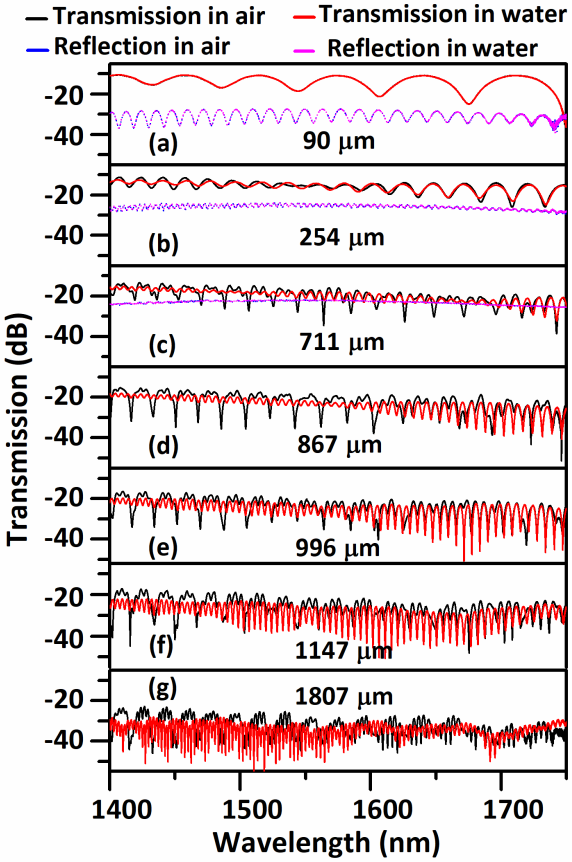

Fig. 3. Measured spectral responses in air and water of the proposed HCF structure with various HCF-10 lengths.

It has been demonstrated that strength of the resonant dip produced by ARROW is highly dependent on the refection coefficient at the interface between the silica cladding and outer environment, a small change in the reflection coefficient could introduce a significant change in ARROW dip strength [22-23]. The resonant dips disappear when the sensor head is totally immersed in water as shown in Fig. 3, indicating that water is in favor of inhibiting the leakage of energy at resonant wavelengths. Similar results were also demonstrated in our previous work where HCF-30 was used [14]. Figure 4 shows the experimentally measured FSRs in water at different HCF lengths, the measured data have a very good linear response versus *1/L* with a coefficient of 0.9998, which matches very well with the theoretical prediction using Eq. (5). In addition, according to Eq. (5), Δn_{eff} is estimated to be ~0.4342, which confirms the transmission dips are introduced by the interferences between light propagating in the silica cladding (n_{clad} =1.45) and in the air core (n_{core} =1.0). It is thus concluded that the observed transmission dips in water are a result of MZI. It is also found that more stronger MZI dips are emerging and gradually moving to a shorter wavelength with an increase in the HCF length (Fig. 3), thus the hybrid transmission spectrum in air at different wavelength range is significant affected by the MZI effect depending on the HCF length.

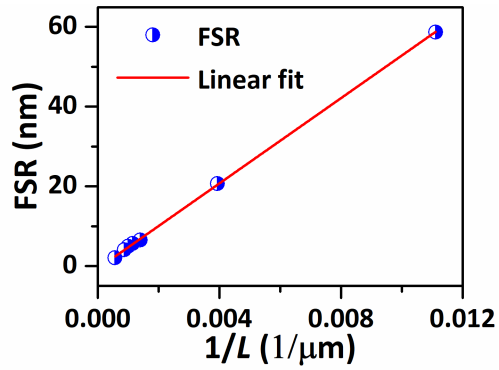

Fig. 4. Experimentally measured FSRs for different lengths of HCF versus *1/L* in water.

Figure 5(a) shows an example of the simulated transmission spectrum of the proposed HCF-10 structure with an HCF length of 800 μm using a beam propagation method (BPM). Periodic strong transmission dips and small ripples are observed, which matches well with the experimental results. The strong dips are excited by ARROW guiding mechanism while the small ripples are produced by MZI, which can be identified from their FSRs. Fig. 5(b) compares the energy distribution along the HCF at an AR wavelength (~1525 nm) and a resonant wavelength (~1538 nm). When light incident into the HCF from the lead in SMF, most of the transmission light propagates in the HCF core while a portion of the light is coupled into the silica cladding. It is evident that light interferences occur within the HCF. At an AR wavelength, light guides in the air core by means of both ARROW and MZI, thus more light energy is confined in the air core. At a resonant wavelength, light guiding through ARROW mechanism is leaking out into the cladding and environment, leaving only MZI guided light in the air core. A longer HCF leads to a higher loss in transmission which agrees well with the experimental results shown in Fig. 3.

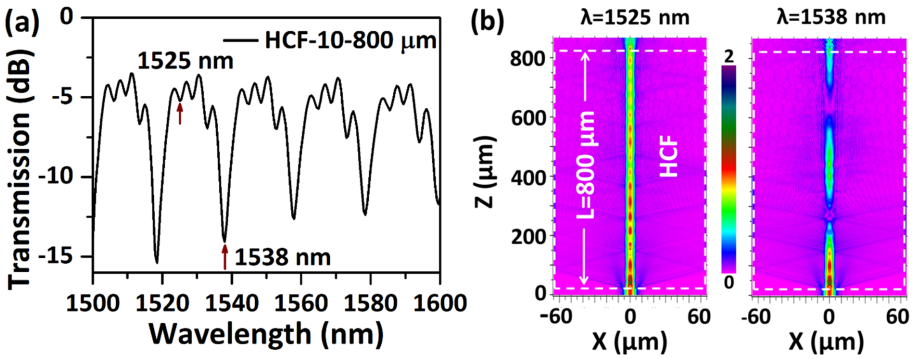

Fig. 5. (a) Simulated transmission spectrum of HCF-10 structure with an HCF length of 800 µm and (b)Simulated energy distribution in the XZ plane along the longitude direction of the SMF-HCF-SMF structure simulated with a BPM at an AR wavelength (1525 nm) and a resonant wavelength (1538 nm).

Since the transmission dips produced by ARROW and MZI have different sensitivities to temperature and strain [24-25], the proposed HCF-10 structure in air could be potentially used as a dual parameter sensor for simultaneous measurement of temperature and strain by employing a characteristic matrix approach, which is under investigation.

4. Results and discussion

Sensor samples S-711, S-867 and S-1147 were chosen for the demonstration of water level measurement (RI=1.3333). When the HCF is partially covered in water then some of the HCF is surrounded by air and some by water. The reflection coefficients at the point where the surrounding medium changes from air to water also change, resulting in a change of the transmitted light intensity at the end of the HCF and consequently in a change of the spectral dip strength. More detailed working principle can be found in our previous work [14]. The dips' strength variations at ~1488.1 nm for S-711, ~1485.5 nm for S-867, and ~1583.7 nm for S-1147 with the increase of the water level were each measured four times to demonstrate the measurement repeatability of the sensors and the results are shown in Fig. 6. Since the resonant dips of the selected sensor samples were strongly modulated by the MZI dips at a longer wavelength, the resonant dips at a relatively short wavelength were easier to identify and the resonant dip with relatively large extinction ratio was preferred and chosen for the liquid level measurement for S-711 and S-867. However with the increase of the HCF length, the resonant dips split due to the increase of the transmission loss and a more significant modulation from the MZI dips. Thus a dip with a relatively large extinction ratio changes between air and water was chosen for the liquid level measurement for S-1147. Figure 6 (a) shows an example of the measured transmission spectral responses for S-867 at various water levels. The resonant dips are found to have no central wavelength shift with an increase in the liquid levels but only experience changes in the dip strength [14]. In this work however a small dip shift is observed which is introduced by the shift of MZI dips. The sensor structure has a very good performance in the repeatability test as shown in Fig. 6(b). The sensor sample with a longer HCF length offers a better sensitivity to changes in the liquid level. However, larger dip strength fluctuations were observed when the liquid was covering the start and end portions of the HCF, for the sensor sample with a longer HCF length. These fluctuations are attributed to the modulation from the MZI dips and they are only observed at the start and end portions of the HCF since the sensor has a much higher sensitivity in the middle portion of the HCF [14]. This problem could be solved by separating the start and end portions of the HCF from the liquid flow channel in the packaging system.

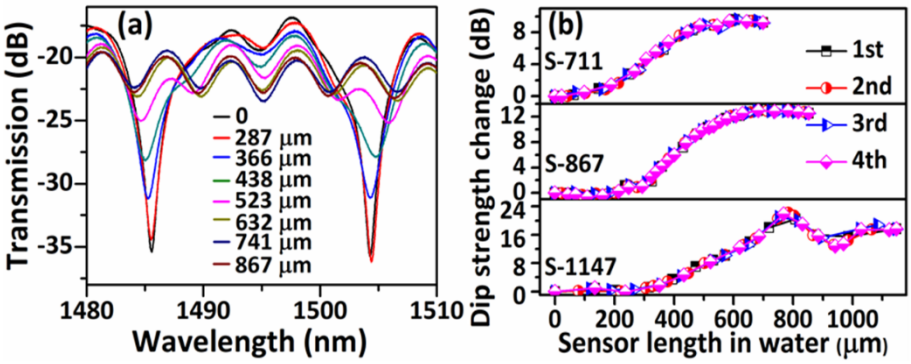

Fig. 6. (a) Examples of measured spectral responses for S-867 and (b) four times repeated measurement of dips' strength changes of HCF based sensor samples with different lengths of HCF at different water levels.

Given that the central aim of this work was fabrication of a micrometer length liquid level sensor for microfluidic applications, and since S-867 had a good balance between the transmission loss and sensitivity, it was subsequently used for a more detailed investigation of its performance in different RI liquids. Figure 7 summarizes the dips' strength variations in a range of RI liquids versus the length of the sensor coved in liquid, with each liquid tested four times. It can be seen that the change of the SRI within the range from 1.3333 to 1.3720 has little influence on the dip strength, which gives the proposed sensor structure a big advantage against the previously reported liquid level sensors which suffer from a high cross sensitivity to changes in the SRI. The highest sensitivity to liquid level change is obtained in the range from ~300 µm to ~500 µm, the measured data of this range and their linear fit are shown in the inset figure of Fig. 7(b). The calculated best liquid level sensitivity in this liquid level range is ~0.042 dB/µm, which corresponds to a liquid level measurement resolution of ~0.23 µm assuming the OSA has an intensity resolution of 0.01 dB. This is the highest liquid level sensitivity reported to date based on intensity modulation. In particular, it is 14 times higher than tilted fiber grating structure and three times higher than our previously reported AR HCF structure [6, 14]. It is noted that such an ARROW structure could be imprinted directly inside a microfluidics device to realize a more robust device with a high level of photonic-liquid integration [26].

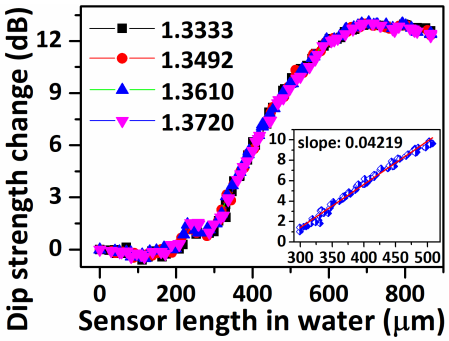

Fig. 7. Measured dip strength changes at ~1485.5 nm during liquid level measurement for a number of liquid SRI values. The inset figure shows the measured data for all liquids in the HCF length range from 300 µm to 500 µm and their linear fit.

5. Conclusion

In conclusion, a micrometer length HCF structure is proposed for high sensitivity liquid level measurement with sub-micrometer resolution for microfluidic applications. HCFs with different air core diameters (10 μm, 20 μm, 30 μm) were investigated and it is found that for a given length of HCF stronger resonant dips were excited in transmission for the HCF with a smaller air core diameter. HCF-10 is thus chosen for a detailed investigation on light transmission mechanism and liquid level measurement. It is found that both ARROW and MZI guiding mechanism were excited in the HCF structure when the HCF was longer than the critical length. A maximum sensitivity of 0.042 dB/μm was experimentally demonstrated for the sensor with an HCF-10 length of 867 μm which is three times higher than that of the previously reported fiber optic liquid level sensors based on intensity modulation. The estimated liquid level measurement resolution is ~0.23 μm. In addition, the proposed sensor structure is demonstrated with good repeatability and a very low cross sensitivity to changes in the SRI.

Acknowledgments

This work was financially supported by the Guangdong Basic and Applied Basic Research Foundation (2019A1515110320); Shenzhen Basic Research Foundation (JCYJ20190808173401660, JCYJ20190808140805488, JCYJ20190808173619062); China Postdoctoral Science Foundation (2019M663025); National Natural Science Foundation of China (11874332); National major scientific research instrument development project of Natural Science Foundation of China (61727816); Department for Agriculture, Food and the Marine, Ireland (17F284).

Disclosures. The authors declare no conflicts of interest.

References

[1] M. Joanicot and A. Ajdari, “Droplet Control for Microfluidics,” Science, **309**, 887-888 (2005).
[2] G. M. Whitesides, “The origins and the future of microfluidics,” Nature, **442**, 368-373 (2006).
[3] N. Khalid, I. Kobayashi and M. Nakajima, “Recent lab-on-chip developments for novel drug discovery,” Wiley Interdiscip. Rev. Syst. Biol. Med. **9**, e1381 (2017).
[4] C. Lin, C. Liao, Y. Zhang, L. Xu, Y. Wang, C. Fu, K. Yang, J. Wang, J. He, and Y. Wang, “Optofluidic gutter oil discrimination based on a hybrid-waveguide coupler in fibre,” Lab Chip, **18**(4), 595-600 (2018).
[5] R. Gao, D. F. Lu, M. Y. Zhang, and Z. M. Qi, “Optofluidic waveguide Immunosensor Based on Resonant Wavelength Shift of a Hollow Core Fiber for Ultratrace Detection of Carcinogenic Benzo[a]pyrene,” ACS Photon. **5**(4), 1273–1280 (2018).
[6] Z. J. Yan, C. B. Mou, Z. Y. Sun, K. M. Zhou, H. S.Wang, Y. S.Wang, W. Zhao, and L. Zhang, “Hybrid tilted fiber grating based refractive index and liquid level sensing system”, Opt. Commun. **351**(15), 144-148 (2015).
[7] J. E. Antonio-Lopez, J. J. Sanchez-Mondragon, P. LiKamWa, and D. A. May-Arrioja, “Fiber-optic sensor for liquid level measurement,” Opt. Lett. **36**(17), 3425–3427 (2011).
[8] J. Wang, Q. Sun, Y. Li, S. Tan, L. Yang, F. Fang, Z. Yan, and D. Liu, “Highly sensitive liquid-level sensor based on an optical reflective microfiber probe”, Opt. Lett. **45**(1), 169-172 (2020).
[9] H.Y. Fu, X.W. Shu, A.P. Zhang, W.S. Liu, L. Zhang, S.L. He, and I. Bennion, “Implementation and characterization of liquid-level sensor based on a long-period fiber grating Mach–Zehnder interferometer,” IEEE Sens. J. **11**, 2878-2882 (2011).
[10] S.M. Chandani, N.A.F. Jaeger, “Optical fiber-based liquid level sensor,” Opt. Eng. **46**(11), 114-401 (2007).
[11] B. Yun, N. Chen, and Y. Cui, “Highly sensitive liquid-level sensor based on etched fiber bragg grating,” IEEE Photon. Technol. Lett. **19**(21), 1747–1749 (2007).
[12] H. Gong, H. Song, S. Zhang, K. Ni, X. Dong, “An optical liquid level sensor based on polarization-maintaining fiber modal interferometer,” Sensor Actuat. A: Phys. **205**, 204-207 (2014).
[13] K. R. Sohn, and J. H. Shim, "Liquid-level monitoring sensor systems using fiber Bragg grating embedded in cantilever", Sens. Actuator A: Phys. **152**, 248-251 (2009).
[14] D. Liu, F. Ling, R. Kumar, A. K. Mallik, K. Tian, C. Shen, G. Farrell, Y. Semenova, Q. Wu, and P. Wang, “Sub-micrometer resolution liquid level sensor based on a hollow core fiber structure”, Opt. Lett. **44**(8), 2125-2128 (2019).
[15] N. M. Litchinitser, A. K. Abeeluck, C. Headley, and B. J. Eggleton, “Antiresonant reflecting photonic crystal optical waveguides,” Opt. Lett. **27**(18), 1592–1594, 2002.
[16] X. Zhang, H. Pan, H. Bai, M. Yan, J. Wang, C. Deng, and T. Wang, “Transition of Fabry-Perot and antiresonant mechanisms via a SMF-capillary-SMF structure,” Opt. Lett. **43**(10), 2268–2271 (2018).

[17] Y. Jung, S. Lee, B. H. Lee, and K. Oh, "Ultracompact in-line broadband Mach-Zehnder interferometer using a composite leaky hollow-optical-fiber waveguide," Opt. Lett. **33**(24), 2934–2936 (2008).
[18] C. Wei, R. J. Weiblen, C. R. Menyuk, and J. Hu, "Negative curvature fibers," Adv. Opt. Photon. **9**(3), 504–561 (2017).
[19] B. H. Lee, and J. Nishii, "Dependence of fringe spacing on the grating separation in a long-period fiber grating pair," Appl. Opt. **38**(16), 3450-3459 (1999).
[20] M. S. Ferreira, L. Coelho, K. Schuster, J. Kobelke, J. L. Santos, and O. Frazao, "Fabry–Perot cavity based on a diaphragm-free hollow-core silica tube," Opt. Lett. **36**(20), 4029–4031 (2011).
[21] C. R. Liao, D. N. Wang, and Y. Wang, "Microfiber in-line Mach-Zehnder interferometer for strain sensing," Opt. Lett. **38**(5), 757–759 (2013).
[22] D. Liu, R. Kumar, F. Wei, W. Han, A. K. Mallik, J. Yuan, C. Yu, Z. Kang, F. Li, Z. Liu, H.-Y. Tam, G. Farrell, Y. Semenova, and Q. Wu, "Highly sensitive twist sensor based on partially silver coated hollow core fiber structure," J. Lightwave Techno. **36**(17), 3672-3677 (2018).
[23] S. Liu, J. Tian, N. Liu, J. Xia, and P. Lu, "Temperature insensitive liquid level sensor based on antiresonant reflecting guidance in silica tube," J. Lightwave Technol. **34**(22), 5239–5243 (2016).
[24] D. Liu, Q. Wu, C. Mei, J. Yuan, X. Xin, A.K. Mallik, F. Wei, W. Han, R. Kumar, C. Yu, S. Wan, X. He, B. Liu, G.-D. Peng, Y. Semenova, G. Farrell, "Hollow Core Fiber Based Interferometer for High Temperature (1000 °C) Measurement", J. Lightwave Techno. **36**(9), 1583-1590 (2018).
[25] W. Ni, P. Lu, J. Zhang, C. Yang, X. Fu, Y. Sun, H. Liao, and D. Liu, "Single hole twin eccentric core fiber sensor based on anti-resonant effect combined with inline Mach-Zehnder interferometer," Opt. Express, **25**(11), 12372-12380 (2017).
[26] H. Schmidt, D. Yin, D. W. Deamer, J. P. Barber and A. R. Hawkins, "Integrated arrow waveguides for gas/liquid sensing," Proc. SPIE, **5515**, 67–80 (2004).